

Single-Atom Switches and Single-Atom Gaps Using Stretched Metal Nanowires

Qingling Wang,^{†,||} Ran Liu,^{‡,||} Dong Xiang,^{*,†} Mingyu Sun,[†] Zhikai Zhao,[†] Lu Sun,[†] Tingting Mei,^{†,§} Pengfei Wu,[†] Haitao Liu,[†] Xuefeng Guo,[⊥] Zong-Liang Li,^{*,‡} and Takhee Lee^{*,§}

[†]Key Laboratory of Optical Information Science and Technology, Institute of Modern Optics, College of Electronic Information and Optical Engineering, Nankai University, Tianjin 300071, China

[‡]College of Physics and Electronics, Shandong Normal University, Jinan 250014, China

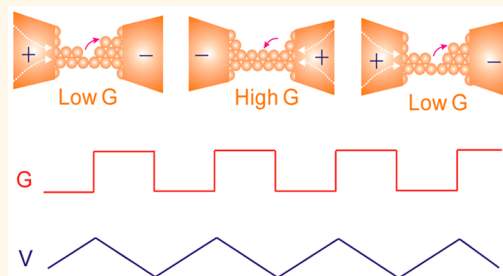
[§]Department of Physics and Astronomy, and Institute of Applied Physics, Seoul National University, Seoul 08826, Korea

[⊥]Beijing National Laboratory for Molecular Sciences, College of Chemistry and Molecular Engineering, Peking University, Beijing 100871, China

Supporting Information

ABSTRACT: Utilizing individual atoms or molecules as functional units in electronic circuits meets the increasing technical demands for the miniaturization of traditional semiconductor devices. To be of technological interest, these functional devices should be high-yield, consume low amounts of energy, and operate at room temperature. In this study, we developed nanodevices called quantized conductance atomic switches (QCAS) that satisfy these requirements. The QCAS operates by applying a feedback-controlled voltage to a nanoconstriction within a stretched nanowire. We demonstrated that individual metal atoms could be removed from the nanoconstriction and that the removed metal atoms could be refilled into the nanoconstriction, thus yielding a reversible quantized conductance switch. We determined the key parameters for the QCAS between the “on” and “off” states at room temperature under a small operating voltage. By controlling the applied bias voltage, the atoms can be further completely removed from the constriction to break the nanowire, generating single-atom nanogaps. These atomic nanogaps are quite stable under a sweeping voltage and can be readjusted with subangstrom accuracy, thus fulfilling the requirement of both reliability and flexibility for the high-yield fabrication of molecular devices.

KEYWORDS: molecular electronics, quantized conductance switches, electromigration, nanogaps, molecular devices, single-atom memory



With the rapid development of semiconductor technologies, the feature size of electronic devices is gradually approaching the miniaturization limit of silicon-based technology. Today, a single atom or single molecule may represent the ultimate limit of what can be achieved.^{1,2} The practice of utilizing individual molecules as functional units in electronic devices has quickly promoted the development of nanotechnology, and many significant results have been obtained.^{3–16} However, the fabrication of molecular devices fulfilling the requirements of high-yield, room-temperature operability and low energy consumption still faces great challenges. For example, we previously reported the effective molecular orbital gating of single molecular transistors using the electromigration technique.¹⁷ However, to promote the application of the device, the yield of molecular device fabrication (~1%) should be improved; the need for improvement originates from the fact that the gap size between two electrodes cannot match the molecular length exactly when the electromigration technique is employed to break the gold wires

to generate gaps. The motion of metal atoms caused by the electromigration process is too fast to be precisely controlled for a bulk metal wire with a diameter of 100 nm, and the gap size may randomly fall between 1 and 100 nm, which is normally larger than the molecular dimensions, leading to a low yield of molecular junctions.

To solve this low-yield problem, we developed a reliable methodology that combines the mechanically controllable break junction (MCBJ) technique¹⁸ with the electromigration technique¹⁷ to generate sub-nanometer gaps between electrodes. In this strategy, a metal wire with a constriction is mechanically stretched to a few atoms in thickness followed by a feedback-controlled electromigration process. We demonstrated that the atomic motion process can be slowed down

Received: August 23, 2016

Accepted: October 5, 2016

Published: October 5, 2016

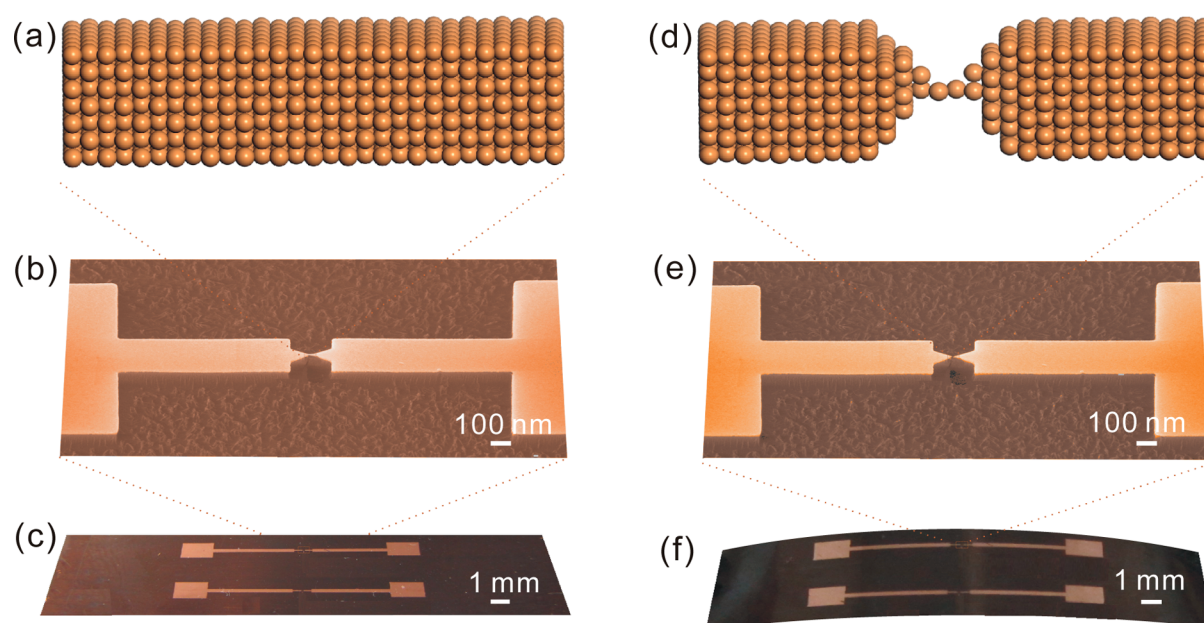


Figure 1. MCBJ chips before and after stretching. (a) Schematic diagram of the atomic metal wire before stretching. (b) Scanning electron microscopy (SEM) image of a nanofabricated MCBJ chip. (c) Optical image of the MCBJ chip. Two parallel junctions with central constrictions were fabricated on a spring steel substrate. (d) Schematic diagram of the atomic metal wire after stretching. (e) SEM image of a nanofabricated MCBJ chip after bending the substrate. (f) Optical image of the MCBJ chip after bending the substrate. The chip was mounted in a three-point bending configuration. The push rod (motor actuated) exerts a bending force on the substrate. The bending force stretches the metal wire at the smallest constriction.

dramatically, a behavior distinguishable from that of bulk nanowires. With the last atom removed from the constriction, *i.e.*, the nanowire is completely broken, gaps on a scale of a few metal atoms (less than 1.0 nm) are generated. These gaps are found to be quite stable under a sweeping voltage, unlike those fabricated by the MCBJ method alone. These gaps can be further mechanically adjusted with picometer accuracy to match the molecular length, which would enhance the yield of molecular junctions. Furthermore, it is intriguing that the conductance of the nanowire before being completely broken can be switched between two defined quantized values as a two-way bias voltage is applied. Combining real-time conductance measurements and *ab initio* calculations, we provide evidence that the quantized conductance switching results from atom dislocation induced by current, proving that single-atom switches employing a stretched nanowire can be realized at room temperature.

RESULTS AND DISCUSSION

Metal Nanowire Stretching. A critical step to realizing an atomic switch in our experiment is the precise control of the stretching of metal wires. In this study, we employed the MCBJ technique to precisely stretch metal wires with subangstrom accuracy.^{19–28} To achieve high mechanical stability and make the nanowire insensitive to external vibration, (1) we employed electron beam lithography rather than traditional optical lithography to fabricate the suspended nanowires and (2) used differential screws instead of a single screw to generate a variable force to precisely stretch nanowires; thus, the attenuation factor was significantly enhanced. The calculated attenuation factor (r) for our setup is $r \sim 2 \times 10^{-6}$, which, to the best of our knowledge, is the smallest value reported. In addition, we (1) replaced the piezo actuator with a vacuum-compatible motor to drive and lock-in the push rod and (2)

prehardened the insulation layer under vacuum to prevent deformation during the experiment. Through these optimizations, unexpected vibrations and the drift in the gap size were suppressed (Figures S1–S4). The final fabricated chip is shown in Figure 1a–c.

We chose gold wire as our target material because (1) the high ductility of gold upon stretching makes it suitable as an atomic-scale metal wire in the MCBJ technique, (2) gold is the most frequently used metal in the fabrication of devices by electromigration and can be easily patterned by well-established nanofabrication techniques such as electron-beam lithography, and (3) gold possesses stable chemical properties; for instance, it is a noble metal, preventing oxidation.

When the push rod exerted a bending force on the substrate, the constriction part underwent the largest stretching force, which reduced the cross section of the constriction, as shown in Figure 1d,e. We precisely stretched the metal wire at a speed of 0.1 Å/step at 0.1 bar, and the conductance was monitored simultaneously. A pressure of 0.1 bar was achieved by repeating this bumping/refilling process within several cycles. Once the conductance was near $1 G_0$ ($G_0 = 2 e^2/h$, corresponds to the single gold atom conductance), the push rod was fixed in a “lock-in” state by holding the driven motor. It is noteworthy that the conductance was stable without obvious fluctuations over several hours when the push rod was fixed at such middle vacuum pressure, and no “self-breaking” was observed, distinguishable from the previous report with the piezo component as push rod due to the unexpected drift of the piezo.^{18,29} See Figure S5 in the Supporting Information for detailed information.

Switching Behavior of Quantized Conductance. A voltage was subsequently applied to the nanowire to induce the electromigration process with a fixed push rod under middle pressure (0.1 bar). This middle pressure was achieved by

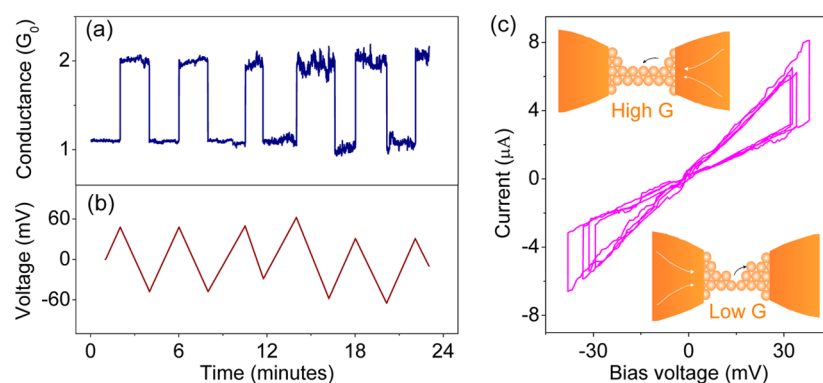


Figure 2. Conductance switching upon programmed biases and memory behavior during a programmed voltage sweeping process. (a) Conductance of a break junction as a function of time when a program-controlled bias was applied. (b) Feedback-controlled voltage was applied to the source and drain electrodes. (c) I – V curves during the cycled voltage sweeping process. The voltage was initially swept from 0 V to positive values. Inset: Schematic illustration of the reversible atom migration when the passing current was reversed.

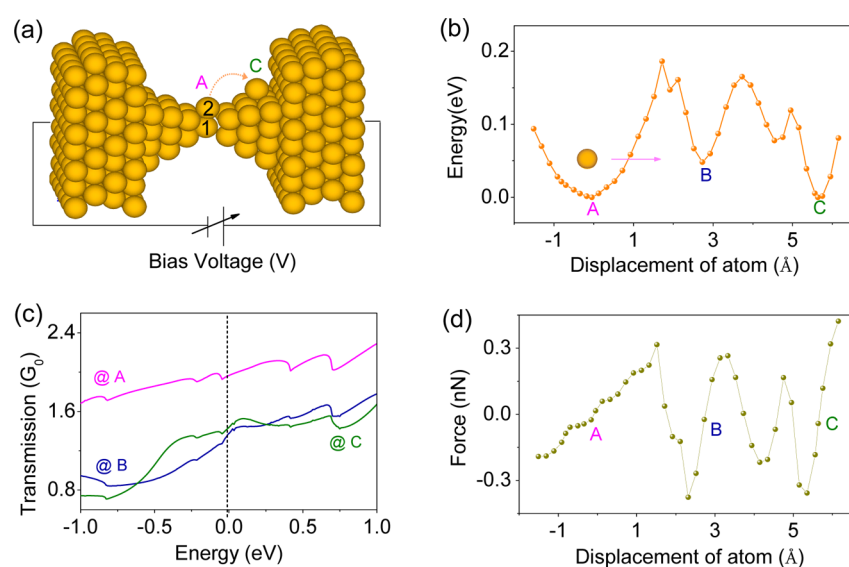


Figure 3. *Ab initio* calculation of atom migration process. (a) Model for the calculation. In configuration B, the migrating atom Au 2 is located at the hollow position of the migration path from A to C. (b) Energy curve for the migration of single gold atom Au 2. (c) Transmission spectra for atom Au 2 at points A, B, and C, respectively. The dashed line indicates the Fermi level. (d) Force curve for atom Au 2 migrating on the gold surface.

repeatedly bumping out the gas from the MCBJ chamber and refilling the chamber with argon. To slow the electromigration process, a feedback-controlled system was employed^{27,30} in which the applied voltage was actively adjusted in response to the conductance change. Once a conductance jump ($>0.2 G_0$) was detected, a linear decrease in the voltage was triggered and controlled by the feedback system immediately. We found that the conductance of this junction could be switched between two defined quantized values [$1 G_0$, $2 G_0$] when the voltage amplitude was linearly decreased to zero and subsequently swept in the reverse direction. Figure 2 shows a typical quantized conductance switch upon the application of a programed bias voltage between -60 and $+60$ mV. A conductance switch in the other region, such as [$2 G_0$, $6 G_0$] with a preferred jump height of $\sim 1 G_0$, was also observed, as shown in Figure S6 in the Supporting Information.

To gain insight into the quantized conductance behavior of the switch, we further performed current–voltage (I – V) measurements with a programed sweeping bias voltage. The voltage was initially swept linearly in one direction, and once a

current jump was detected, the voltage sweeping direction was reversed. Figure 2c presents typical I – V curves during the cyclic processes. As shown, the I – V curves mainly fall into two slots. Differentiation of these I – V curves shows that the conductance value switched between $\sim 1 G_0$ and $\sim 2 G_0$. This observation is coherent with the quantized conductance switch behavior.

The quantized conductance switch was attributed to atomic motion driven by the current. Upon stretching, the nanowire was elongated, which led to a rearrangement of gold atoms in the constriction; e.g., the mechanical stretching or recontact may have pushed the inner metal atoms to the surface, causing the electrode surface to no longer be smooth.^{31,32} The gold atoms on the edge of the constriction region possessed the minimum number of nearest neighbors, placing these atoms in an “unstable state”. These atoms at the edge experienced a strong force induced by the current:³³ (1) the direct force exerted by the action of the electrical field onto the ions and (2) the so-called wind force due to the momentum transferred from the traveling electrons to the atoms. Several pioneering theoretical works claimed that current-induced forces during

electromigration should be sufficient to overcome the energy barriers to breaking Au–Au bonds and triggering the motion of gold atoms.^{30,34} Following these studies, we performed detailed calculations to confirm our atomic motion hypothesis.

Theoretical Calculations for Atomic Motion. To verify our atomic motion assumption and better understand the mechanism for this conductance switching behavior, we carried out a series of *ab initio* calculations to simulate the stretching process of gold wires and analyze the migration of a single gold atom. The simulations show that repeatedly breaking and reforming gold bridges can create various contact geometries, as previously reported.^{35,36} An adapted model in which the two electrodes are initially connected by two gold atoms (Au 1, Au 2) is shown in Figure 3a. Au 1 is connected to two electrodes *via* a hollow site, and Au 2 protrudes slightly from the electrode surface. See Figure S7 in the Supporting Information for more details.

Figure 3b shows the energy curve of the system with the migrating gold atom Au 2 located at different positions along the gold surface. Configuration A corresponds to the initial state in which Au 2 is located at the top of Au 1 and a double-conductance channel is formed. Point B corresponds to the state in which Au 2 is located in a hollow position in the migration path, and C corresponds to Au 2 located near the right corner position. Figure 3b shows that the energy of configuration C is similar to that of A but is approximately dozens of meV lower than that of B. The potential barrier between points A and B is approximately 200 meV, which prevents Au 2 from spontaneously migrating away from point A. At room temperature, Au 2 generally possess vibration energy ($1 k_B T \sim 2 k_B T$, *i.e.*, 26–52 meV), and Au 2 may obtain additional vibration energy from neighboring atoms. This vibration energy assists atom motion but is still not sufficient to overcome the 200 meV barrier without the help of a bias voltage. Although the thermal vibration contributes the majority of the energy for surface gold atom migration, we believe that the bias voltage dominates atomic migration because thermal vibration mainly causes motions near the equilibrium position and in random directions, whereas the bias voltage can drive a surface gold atom along a specific direction. If the energy gained from an applied bias is comparable or greater than dozens of meV, the atom can migrate to point B and subsequently to C with the help of atomic vibrations at room temperature.³⁷ Based on this calculation, there should be a threshold voltage of approximately dozens of mV for atom migration, which agrees with our experimental observation. Because configurations A and C have similar energy, the system may possess bistable states, which make conductance switching feasible. In addition, considering the Boltzmann distribution law, Au 2 has the chance to be thermally excited to high vibration states; thus, spontaneous migration seems inevitable. However, high excited vibration states may be suppressed by exchanging phonons with the surrounding gas; thus, one can expect that inert gases with a certain gas pressure will suppress the spontaneous thermal migration of surface gold atom efficiently. This matter will be discussed in detail in the Discussion.

Figure 3c shows the transmission spectra for the different configurations during atom migration. The figure demonstrates that the transmission spectrum for configuration A is clearly higher than the spectra for configurations B and C. The transmission spectra indicate that the conductance of the junction will decrease sharply as atom migration starts (*e.g.*, A

→ B), and then the conductance should be stable with small fluctuations in the following migration process (*e.g.*, B → C). Additionally, it can be observed that the transmission value near the Fermi level for configuration A is approximately $2 G_0$ and the transmission value for configuration B or C is close to $1 G_0$, which agrees with our experimental observation. Figure 3d shows the force required for atom migration along the electrode surface. The figure demonstrates that the force is discrete during atomic migration and the maximum force for atom migration is approximately 0.4 nN. This relatively low force makes it easy for atom migration to occur, and the discrete force also makes it feasible to slow the migration process. Therefore, the energy curves, the transmission spectra, and the force curves indicate that controlling atom migration on the single-atom level is feasible, and the conductance switch should be caused by the atom dislocation process.

Generation of Single-Atom Gaps. Following the foregoing theoretical explanation, an atomic-sized gap will appear if a one-way voltage is applied until the last atom is removed from the constriction regime. To confirm this assumption, we applied a one-way voltage to a nanowire whose conductance was a few G_0 . Figure 4 shows the conductance changes as a

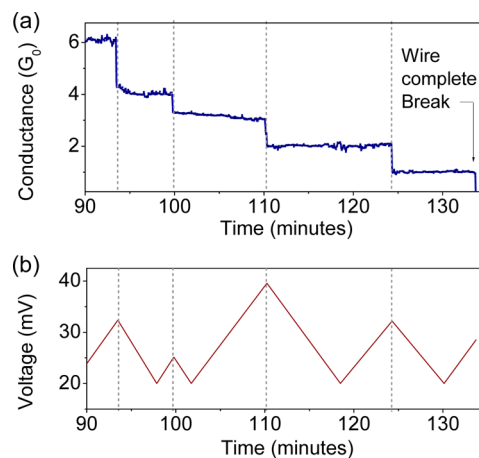


Figure 4. Conductance evolution upon a programmed bias voltage as a function of time. (a) Stepwise decrease in conductance upon programmed bias until a complete breaking of the junction. (b) Feedback-controlled voltage applied to source–drain electrodes. Once a conductance jump ($>0.2 G_0$) is detected, the bias voltage is reduced automatically to slow down the atom migration process until it reaches the preset bottom voltage (20 mV), after which the bias voltage was triggered to increase again.

function of the applied voltage. Please note that the sweeping direction of the applied voltage was never changed, but the amplitude of the applied voltage was programmed to decrease once a conductance jump was detected. When the decreasing voltage reached the threshold voltage (it was preset to 20 mV), the bias voltage was set to increase again. Interestingly, a stepwise quantized conductance decrease (integer multiple of G_0) was clearly observed (discrete conductance steps were also observed after molecular adsorption onto the gold wires, as shown in Figure S8, which will be further addressed in the future). When the last atom that bridged the nanowire was finally removed from the constriction, the current jumped to the tunnel regime, indicating the complete breaking of the nanowire, and an atomic-scale gap was generated.

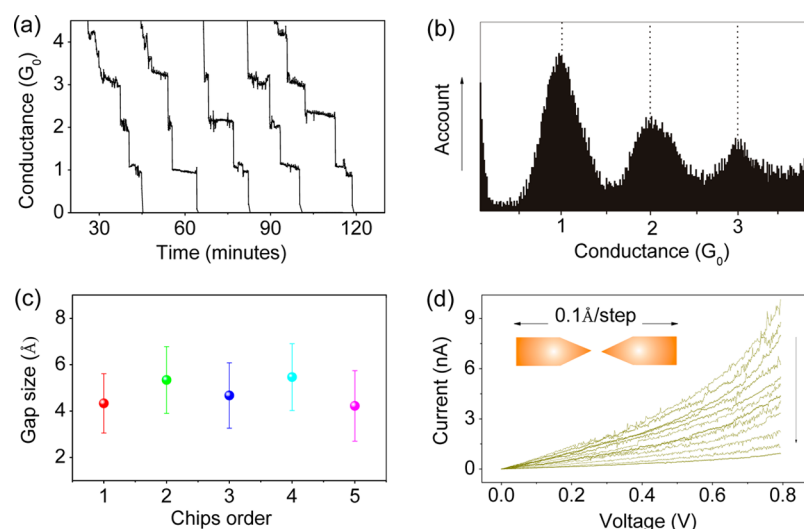


Figure 5. Junction conductance evolution upon a programmed bias voltage and the characterization of gap size after complete breaking of the junctions. (a) Conductance of the gold contact decreased in quantum steps near multiples of G_0 when the programmed bias voltage (as illustrated in Figure 2b) was applied to the junction. (b) Corresponding conductance histogram constructed from 452 conductance curves, showing well-defined peaks centered at $1 G_0$, $2 G_0$, and $3 G_0$. (c) Average distribution of the gap size for five chips. (d) $I-V$ curves obtained as the gap size was readjusted at $0.1 \text{ \AA}/\text{step}$.

A major merit of the MCBJ technique is that the separated electrodes can be brought back into contact again and then broken once more, which means that many test samples can be obtained from a single chip. Hence, we performed a statistical analysis of the steplike conductance curves. Among all tested samples, approximately 70% (301 out of 452 samples) clearly demonstrated a discrete decrease in conductance upon the application of a programmed bias voltage, as shown in Figure 5a. In other words, the conductance traces decreased in a stepwise fashion, and each step occurred preferentially at an integer multiple of the conductance quantum G_0 . A histogram constructed from these 452 conductance curves shows pronounced peaks at $1 G_0$, $2 G_0$, and $3 G_0$, as shown in Figure 5b, demonstrating the well-known quantization of conductance.^{38,39}

After the metal wire was broken, two separated nanoelectrodes were generated and the gap between the two electrodes was subsequently calculated precisely (see Figure S9 in the Supporting Information). We found that the gap size mainly falls into two regions, as shown in Figure S10 in the Supporting Information. One region spans from 3.0 to 4.2 Å, which is similar to the diameter of a single gold atom. The other spans from 5.8 to 7.2 Å, which is comparable to the size of two gold atoms. We examined five different chips (numbered as chips 1–5), and each was used to generate approximately 15 gaps repeatedly. The average gap size and uncertainty data measured with these junctions are depicted in Figure 5c. As shown, the gap sizes were on the scale of a few atoms, indicating that the method combining MCBJ with the electromigration technique is useful for fabricating atom-sized gaps and even single-atom gaps.

These atomic gaps can be mechanically readjusted to match the dimension of target molecules, thus enhancing the yield of small molecular junctions. Due to the amazing attenuation factor, the gap size only increased/decreased by 0.1 \AA as the push rod, driven by a motor, rotated by approximately 90° . Thus, we can readjust the gap size with picometer accuracy. Figure 5d shows a series of $I-V$ curves obtained as the gap size was increased by $0.1 \text{ \AA}/\text{step}$ by the driving motor. One

impressive feature of these $I-V$ curves is that they are stable; *i.e.*, little fluctuation was observed. Normally, at room temperature, the $I-V$ curves show distinct fluctuation during the voltage-sweeping process when the nanogaps are obtained solely by mechanically breaking nanowires.⁴⁰ Our result indicates that the atom on the electrode tip generated by the electromigration method is more stable than that generated by mechanical stretching. This method for nanogap fabrication fulfills the requirements of both flexibility and stability.

Discussion. Atomic-scale electronic switches have been previously reported.^{2,41–45} Here, we provide several advancements for discussion. First, we found that a proper vacuum condition is key to realizing single-atom switches at room temperature. Single-atom switching was demonstrated by Schirm *et al.*³⁰ This report demonstrated that the conductance state could be controlled by electromigration under cryogenic conditions (below 1 K), and the researchers performed a detailed analysis of the conductance channels involved, combining experiments with simulations. Schirm *et al.* provided an important platform for studying electromigration at the atomic scale. In contrast, we demonstrated that such QCASs can be further operated at room temperature, which should greatly expand the application of this single-atom switch.⁴⁶ It is noteworthy that the QCAS device failed to perform under ambient conditions or under high vacuum. No distinct switching behavior was observed in an ambient environment because (1) the ambient air environment may result in contamination and (2) standard atmospheric pressure can suppress the excitation energy, thus decreasing the contribution of atomic vibrations. The suppression of atomic vibration makes it hard for surface atom across the barrier with a small bias voltage. If a large bias voltage is applied to trigger atom motion, then irreversible atomic rearrangement may occur, which may hinder the reversible switching behavior. We did not observe distinct switching behavior under ultrahigh vacuum, which was attributed to the nondirectional migration of atoms driven by high vibration excitation energy under ultrahigh vacuum. It means random motion of gold atoms may occur under ultrahigh vacuum, which makes it difficult to form a

reversible atom switch. Actually, we observed the self-breaking of the atomic wire under ultrahigh vacuum (Figure S11). We believe that refilling with argon (middle level vacuum ~ 0.1 bar) plays an important role in forming a reversible atomic switch by (1) suppressing contamination because the majority of particles/molecules in the chamber are pumped out, leading to a much cleaner environment compared with ambient air, (2) reducing the diffusion of gold atoms on the electrodes because the intermediate pressure facilitates thermal transfer and creates a pressure-induced force, and (3) allowing argon to exchange phonons with the surface gold atoms and suppressing the high excited vibration mode and further preventing spontaneous thermal diffusion. Therefore, we claim that the middle pressure achieved with refilled inert gas is a key parameter for forming the atomic switch at room temperature. We also believe that the chemical nature and the mobility of gold atoms play an important role in determining the rearrangement of single atoms. A further deep experiment with system varied materials is deserved to reveal the effects of metallic elements on atomic motion.

A second advancement is that, by combining experiments and simulations, we provide evidence that the movement of a single atom can result in quantized conductance switching. In particular, we demonstrate that individual metal atoms can be removed from the constriction, and the removed atoms can be refilled in the constriction. Using real-time TEM imaging, Strachan *et al.* demonstrated that gold atoms can be repeatedly removed layer-by-layer during feedback-controlled electromigration.⁴⁷ However, this experiment was performed with bulk wire (100 nm in diameter) in which the electromigration process was too fast to be controlled; thus, the control of single-atom displacement was unavailable. Macroscopically, current-induced force normally gives rise to avalanche-type atomic displacements in bulk wires.⁴⁶ However, at the scale of an atomic junction, current-induced forces should be considered the result of asymmetric corrections to the interatomic bond forces.⁴⁸ Mechanical properties and quantum transport in atomically thin Au wires have been previously investigated.^{49,50} The motion of the atoms could cease after the dislocation of atoms even if the driving current is still applied because (1) the relaxation of local strain by a dislocation of the atom will lead to a decrease in the local electrical field, (2) the force needed for atomic movement to different positions is discrete, *i.e.*, the discrete energy barrier for the movement of an atom to a new position will slow down the atom migration process, and (3) the passing current will be sharply reduced once atom displacement occurs; *i.e.*, the resistance of the junction is automatically increased as the atom is removed, preventing avalanche-type atom migration. To the best of our knowledge, electromigration experiments on the atomic scale remain scarce.³⁰ The system developed in this study appears to be the ideal test bed for fundamental studies of electromigration at the atomic scale at room temperature.

The third advancement is that our experiments offer a method for the fabrication of extremely small gaps, which cannot be formed by the electromigration method alone. Furthermore, we demonstrated that the sizes of the gaps are quite stable under a sweeping voltage, unlike the one generated solely by the MCBJ method. These gaps can be readjusted with sub-angstrom accuracy, thus fulfilling the requirements of both reliability and flexibility for the high-yield fabrication of molecular nanodevices. We performed initial experiments with molecules employing this test platform. We found that

the yield of molecular junctions was approximately 34.5% after self-assembling molecules in the metal junction. The statistical data are presented in Figure S12 in the Supporting Information. It is noteworthy that this yield of molecular junctions is higher than that of molecular junctions prepared by the electromigration method alone ($\sim 1\%$).¹⁷ Moreover, the gap size can be decreased to actively form molecule junctions by relaxing the MCBJ substrate; thus, the yield of molecular junctions can be further enhanced.

CONCLUSIONS

In summary, the removal of metal atoms in sequence from a constriction in a stretched metal wire and the replacement of the removed atoms in the constriction were demonstrated *via* real-time conductance measurements, gap size measurements, and *ab initio* calculations. These findings can assist in the fabrication of extremely small gaps on the scale of a few metal atoms, which will enhance the yield of molecular junctions. Moreover, a quantized conductance switch relying on single-atom dislocation at room temperature was demonstrated, and the underlying mechanism was illustrated. These findings may shed light on the fabrication of highly integrated switch circuits under ambient conditions. Owing to its hysteretic behavior in two distinct states, this switch has the potential to be used as a nonvolatile information storage component, that is, a current-driven single-atom memory at room temperature.

METHODS

The transmission spectra were calculated using density functional theory and the nonequilibrium Green's function method implemented in the TranSIESTA module of the SIESTA package. In the calculation, the improved Troullier–Martins-type norm-conserving pseudopotentials were used to describe the core electrons of Au atoms, and the Perdew–Burke–Ernzerhof generalized gradient approximation was adopted for the exchange–correlation functional.⁵¹ In the transmission calculation, a single- ζ plus polarization basis set was employed for Au atoms.

ASSOCIATED CONTENT

Supporting Information

The Supporting Information is available free of charge on the ACS Publications website at DOI: 10.1021/acsnano.6b05676.

Detailed information concerning the device fabrication, driven motor, chip fabrication, gap size calculation, yield of molecular junctions, *etc.* (PDF)

AUTHOR INFORMATION

Corresponding Authors

*E-mail: xiangdongde@126.com.
*E-mail: lizongliang@sdu.edu.cn.
*E-mail: tlee@snu.ac.kr.

Author Contributions

^{||}Q.W. and R.L. contributed equally to this work.

Notes

The authors declare no competing financial interest.

ACKNOWLEDGMENTS

We appreciate E. Scheer and D. Mayer for fruitful discussions regarding the MCBJ device design. We are grateful for financial support from the National Creative Research Laboratory Program (Grant No. 2012026372) of Korea, the National Natural Science Foundation of China (21303171, 61571242,

and 21225311), the Natural Science Foundation of Shandong Province, China (ZR2013FM006), and the Fundamental Research Funds for the Central Universities of China.

REFERENCES

- (1) Xiang, D.; Wang, X.; Jia, C.; Lee, T.; Guo, X. Molecular-Scale Electronics: From Concept to Function. *Chem. Rev.* **2016**, *116*, 4318–4440.
- (2) Martin, C. A.; Smit, R. H. M.; van der Zant, H. S. J.; van Ruitenbeek, J. M. A Nanoelectromechanical Single-Atom Switch. *Nano Lett.* **2009**, *9*, 2940–2945.
- (3) van der Molen, S. J.; Naaman, R.; Scheer, E.; Neaton, J. B.; Nitzan, A.; Natelson, D.; Tao, N. J.; van der Zant, H.; Mayor, M.; Ruben, M.; Reed, M.; Calame, M. Visions for a Molecular Future. *Nat. Nanotechnol.* **2013**, *8*, 385–389.
- (4) Ratner, M. A Brief History of Molecular Electronics. *Nat. Nanotechnol.* **2013**, *8*, 378–381.
- (5) Quek, S. Y.; Kamenetska, M.; Steigerwald, M. L.; Choi, H. J.; Louie, S. G.; Hybertsen, M. S.; Neaton, J. B.; Venkataraman, L. Mechanically Controlled Binary Conductance Switching of a Single-Molecule Junction. *Nat. Nanotechnol.* **2009**, *4*, 230–234.
- (6) Chen, F.; He, J.; Nuckolls, C.; Roberts, T.; Klare, J. E.; Lindsay, S. A Molecular Switch Based on Potential-Induced Changes of Oxidation State. *Nano Lett.* **2005**, *5*, 503–506.
- (7) Blum, A. S.; Kushmerick, J. G.; Long, D. P.; Patterson, C. H.; Yang, J. C.; Henderson, J. C.; Yao, Y.; Tour, J. M.; Shashidhar, R.; Ratna, B. R. Molecularly Inherent Voltage-Controlled Conductance Switching. *Nat. Mater.* **2005**, *4*, 167–172.
- (8) Lörtscher, E.; Cizek, J. W.; Tour, J.; Riel, H. Reversible and Controllable Switching of a Single-Molecule Junction. *Small* **2006**, *2*, 973–977.
- (9) Liljeroth, P.; Repp, J.; Meyer, G. Current-Induced Hydrogen Tautomerization and Conductance Switching of Naphthalocyanine Molecules. *Science* **2007**, *317*, 1203–1206.
- (10) Jia, C. C.; Ma, B. J.; Xin, N.; Guo, X. F. Carbon Electrode-Molecule Junctions: a Reliable Platform for Molecular Electronics. *Acc. Chem. Res.* **2015**, *48*, 2565–2575.
- (11) Hodgkiss, J.; Zysman-Colman, E.; Higgins, S.; Solomon, G.; Báldea, I.; Samuel, I.; Venkataraman, L.; Wudl, F.; Xu, B.; Venkataraman, R.; Ottosson, H.; Perepichka, D.; Lemmer, U.; Skabara, P.; Mount, A.; Bradley, D. Molecular Electronics: General Discussion. *Faraday Discuss.* **2014**, *174*, 125–151.
- (12) Ivashenko, O.; Bergren, A. J.; McCreery, R. L. Light Emission as a Probe of Energy Losses in Molecular Junctions. *J. Am. Chem. Soc.* **2016**, *138*, 722–725.
- (13) Kim, Y.; Jeong, W.; Kim, K.; Lee, W.; Reddy, P. Electrostatic Control of Thermoelectricity in Molecular Junctions. *Nat. Nanotechnol.* **2014**, *9*, 881–885.
- (14) Kim, B.; Choi, S. H.; Zhu, X. Y.; Frisbie, C. D. Molecular Tunnel Junctions Based on Pi-Conjugated Oligoacene Thiols and Dithiols Between Ag, Au, and Pt Contacts: Effect of Surface Linking Group and Metal Work Function. *J. Am. Chem. Soc.* **2011**, *133*, 19864–19877.
- (15) Bof Bufon, C. C.; Arias Espinoza, J. D.; Thurmer, D. J.; Bauer, M.; Deneke, C.; Zschieschang, U.; Klauk, H.; Schmidt, O. G. Hybrid Organic/Inorganic Molecular Heterojunctions Based on Strained Nanomembranes. *Nano Lett.* **2011**, *11*, 3727–3733.
- (16) Schwarz, F.; Kastlunger, G.; Lissel, F.; Egler-Lucas, C.; Semenov, S. N.; Venkatesan, K.; Berke, H.; Stadler, R.; Lörtscher, E. Field-Induced Conductance Switching by Charge-State Alternation in Organometallic Single-Molecule Junctions. *Nat. Nanotechnol.* **2015**, *11*, 170–176.
- (17) Song, H.; Kim, Y.; Jang, Y. H.; Jeong, H.; Reed, M. A.; Lee, T. Observation of Molecular Orbital Gating. *Nature* **2009**, *462*, 1039–1043.
- (18) Xiang, D.; Jeong, H.; Lee, T.; Mayer, D. Mechanically Controllable Break Junctions for Molecular Electronics. *Adv. Mater.* **2013**, *25*, 4845–4867.
- (19) Kim, Y.; Hellmuth, T. J.; Sysoiev, D.; Pauly, F.; Pietsch, T.; Wolf, J.; Erbe, A.; Huhn, T.; Groth, U.; Steiner, U. E.; Scheer, E. Charge Transport Characteristics of Diarylethene Photoswitching Single-Molecule Junctions. *Nano Lett.* **2012**, *12*, 3736–3742.
- (20) Konishi, T.; Kiguchi, M.; Takase, M.; Nagasawa, F.; Nabika, H.; Ikeda, K.; Uosaki, K.; Ueno, K.; Misawa, H.; Murakoshi, K. Single Molecule Dynamics at a Mechanically Controllable Break Junction in Solution at Room Temperature. *J. Am. Chem. Soc.* **2013**, *135*, 1009–1014.
- (21) Harzmann, G. D.; Frisenda, R.; van der Zant, H. S. J.; Mayor, M. Single-Molecule Spin Switch Based on Voltage-Triggered Distortion of the Coordination Sphere. *Angew. Chem., Int. Ed.* **2015**, *54*, 13425–13430.
- (22) Yelin, T.; Vardimon, R.; Kuritz, N.; Korytar, R.; Bagrets, A.; Evers, F.; Kronik, L.; Tal, O. Atomically Wired Molecular Junctions: Connecting a Single Organic Molecule by Chains of Metal Atoms. *Nano Lett.* **2013**, *13*, 1956–1961.
- (23) Wu, S. M.; González, M. T.; Huber, R.; Grunder, S.; Mayor, M.; Schönenberger, C.; Calame, M. Molecular Junctions Based on Aromatic Coupling. *Nat. Nanotechnol.* **2008**, *3*, 569–574.
- (24) Wagner, S.; Kisslinger, F.; Ballmann, S.; Schramm, F.; Chandrasekar, R.; Bodenstern, T.; Fuhr, O.; Secker, D.; Fink, K.; Ruben, M.; Weber, H. B. Switching of a Coupled Spin Pair in a Single-Molecule Junction. *Nat. Nanotechnol.* **2013**, *8*, 575–579.
- (25) Manrique, D. Z.; Huang, C.; Baghernejad, M.; Zhao, X. T.; Al-Owaedi, O. A.; Sadeghi, H.; Kaliginedi, V.; Hong, W. J.; Gulcur, M.; Wandlowski, T.; Bryce, M. R.; Lambert, C. J. A Quantum Circuit Rule for Interference Effects in Single-Molecule Electrical Junctions. *Nat. Commun.* **2015**, *6*, 6389.
- (26) Tsutsui, M.; Taniguchi, M.; Kawai, T. Single-Molecule Identification Via Electric Current Noise. *Nat. Commun.* **2010**, *1*, 138.
- (27) Parks, J. J.; Champagne, A. R.; Costi, T. A.; Shum, W. W.; Pasupathy, A. N.; Neuscammann, E.; Flores-Torres, S.; Cornaglia, P. S.; Aligia, A. A.; Balseiro, C. A.; Chan, G. K. L.; Abruna, H. D.; Ralph, D. C. Mechanical Control of Spin States in Spin-1 Molecules and the Underscreened Kondo Effect. *Science* **2010**, *328*, 1370–1373.
- (28) Ponce, J.; Arroyo, C. R.; Tatay, S.; Frisenda, R.; Gavina, P.; Aravena, D.; Ruiz, E.; van der Zant, H. S. J.; Coronado, E. Effect of Metal Complexation on the Conductance of Single-Molecular Wires Measured at Room Temperature. *J. Am. Chem. Soc.* **2014**, *136*, 8314–8322.
- (29) Zhou, C.; Muller, C. J.; Deshpande, M. R.; Sleight, J. W.; Reed, M. A. Microfabrication of a Mechanically Controllable Break Junction in Silicon. *Appl. Phys. Lett.* **1995**, *67*, 1160–1162.
- (30) Schirm, C.; Matt, M.; Pauly, F.; Cuevas, J. C.; Nielaba, P.; Scheer, E. A Current-Driven Single-Atom Memory. *Nat. Nanotechnol.* **2013**, *8*, 645–648.
- (31) Wang, D. X.; Zhao, J. W.; Hu, S.; Yin, X.; Liang, S.; Liu, Y. H.; Deng, S. Y. Where, and How, Does a Nanowire Break? *Nano Lett.* **2007**, *7*, 1208–1212.
- (32) Lagos, M. J.; Autreto, P. A. S.; Bettini, J.; Sato, F.; Dantas, S. O.; Galvao, D. S.; Ugarte, D. Surface Effects on the Mechanical Elongation of AuCu Nanowires: De-Alloying and the Formation of Mixed Suspended Atomic Chains. *J. Appl. Phys.* **2015**, *117*, 094301.
- (33) Lodder, A. Electromigration Theory Unified. *Europhys. Lett.* **2005**, *72*, 774–780.
- (34) Brandbyge, M.; Stokbro, K.; Taylor, J.; Mozos, J. L.; Ordejon, P. Origin of Current-Induced Forces in an Atomic Gold Wire: A First-Principles Study. *Phys. Rev. B: Condens. Matter Mater. Phys.* **2003**, *67*, 193104.
- (35) Liu, R.; Bao, D. L.; Jiao, Y.; Wan, L. W.; Li, Z. L.; Wang, C. K. Study on Force Sensitivity of Electronic Transport Properties of 1,4-Butanedithiol Molecular Device. *Acta Phys. Sin.* **2014**, *63*, 068501.
- (36) Jelinek, P.; Perez, R.; Ortega, J.; Flores, F. *Ab Initio* Study of Evolution of Mechanical and Transport Properties of Clean and Contaminated Au Nanowires Along the Deformation Path. *Phys. Rev. B: Condens. Matter Mater. Phys.* **2008**, *77*, 115447.

- (37) Zandbergen, H. W.; Pao, C. W.; Srolovitz, D. J. Dislocation Injection, Reconstruction, and Atomic Transport on {001} Au Terraces. *Phys. Rev. Lett.* **2007**, *98*, 036103.
- (38) Scheer, E.; Agrait, N.; Cuevas, J. C.; Yeyati, A. L.; Ludoph, B.; Martín-Rodero, A.; Bollinger, G. R.; van Ruitenbeek, J. M.; Urbina, C. The Signature of Chemical Valence in the Electrical Conduction Through a Single-Atom Contact. *Nature* **1998**, *394*, 154–157.
- (39) Gruter, L.; Gonzalez, M. T.; Huber, R.; Calame, M.; Schonenberger, C. Electrical Conductance of Atomic Contacts in Liquid Environments. *Small* **2005**, *1*, 1067–1070.
- (40) Yang, Y.; Liu, J. Y.; Feng, S.; Wen, H. M.; Tian, J. H.; Zheng, J. T.; Schöllhorn, B.; Amatore, C.; Chen, Z. N.; Tian, Z. Q. Unexpected Current-Voltage Characteristics of Mechanically Modulated Atomic Contacts with the Presence of Molecular Junctions in an Electrochemically Assisted-MCBJ. *Nano Res.* **2016**, *9*, 560–570.
- (41) Xie, F. Q.; Maul, R.; Augenstein, A.; Obermair, Ch.; Starikov, E. B.; Schön, G.; Schimmel, Th.; Wenzel, W. Independently Switchable Atomic Quantum Transistors by Reversible Contact Reconstruction. *Nano Lett.* **2008**, *8*, 4493–4497.
- (42) Smith, D. P. E. Quantum Point-Contact Switches. *Science* **1995**, *269*, 371–373.
- (43) Terabe, K.; Hasegawa, T.; Nakayama, T.; Aono, M. Quantized Conductance Atomic Switch. *Nature* **2005**, *433*, 47–50.
- (44) Kozicki, M. N. Nanoscale Memory Elements Based on Solid-State Electrolytes. *IEEE Trans. Nanotechnol.* **2005**, *4*, 331–338.
- (45) Valov, I.; Waser, R.; Jameson, J. R.; Kozicki, M. N. Electrochemical Metallization Memories-Fundamentals, Applications, Prospects. *Nanotechnology* **2011**, *22*, 254003.
- (46) van der Molen, S. J. Single-Atom Switches: Toggled with Electrical Current. *Nat. Nanotechnol.* **2013**, *8*, 622–623.
- (47) Strachan, D. R.; Johnston, D. E.; Guiton, B. S.; Datta, S. S.; Davies, P. K.; Bonnell, D. A.; Johnson, A. T. C. Real-Time TEM Imaging of the Formation of Crystalline Nanoscale Gaps. *Phys. Rev. Lett.* **2008**, *100*, 056805.
- (48) Dundas, D.; McEniry, E. J.; Todorov, T. N. Current-Driven Atomic Waterwheels. *Nat. Nanotechnol.* **2009**, *4*, 99–102.
- (49) Xu, B.; He, H.; Tao, N. J. Controlling the Conductance of Atomically Thin Metal Wires with Electrochemical Potential. *J. Am. Chem. Soc.* **2002**, *124*, 13568–13575.
- (50) Rubio-Bollinger, G.; Bahn, S. R.; Agrait, N.; Jacobsen, K. W.; Vieira, S. Mechanical Properties and Formation Mechanisms of a Wire of Single Gold Atoms. *Phys. Rev. Lett.* **2001**, *87*, 026101.
- (51) Perdew, J. P.; Burke, K.; Ernzerhof, M. Generalized Gradient Approximation Made Simple. *Phys. Rev. Lett.* **1996**, *77*, 3865–3868.